Bulletin of the Seismological Society of America, Vol. 96, No. 6, pp. 1–, December 2006, doi: 10.1785/0120060069

Nonlinear Behavior of Soils Revealed from the Records of the 2000 Tottori, Japan, Earthquake at Stations of the Digital Strong-Motion Network Kik-Net

by Olga V. Pavlenko and Kojiro Irikura

Abstract Acceleration records of the Tottori earthquake (6 October 2000), provided by stations of the Digital Strong-Motion Network Kik-Net, show clear evidence of the nonlinearity of soil response at sites located in near-fault zones. In this study, records of the mainshock of the Tottori earthquake are analyzed, and stresses and strains, induced by the strong motion in the upper 100 or 200 m of soil, are reconstructed at sites located within 80 km from the fault plane. For reconstructing stresses and strains, the method is applied, which we developed and used previously for studying the response of soils during the 1995 Kobe earthquake. Nonlinear time-dependent stress–strain relations in the soil layers are estimated based on vertical-array records. A good agreement between the observed and simulated accelerograms of the Tottori earthquake testifies to the validity of the obtained vertical distributions of stresses and strains in the soil layers. We also evaluated variations of the shear moduli of the soil layers, caused by the strong motion, at stations located at different distances from the fault plane. Changes in the rheological properties of the upper soil layers were found closest to the fault-plane stations. A similarity in stress–strain relations, describing the behavior of similar soils during the 1995 Kobe earthquake and the 2000 Tottori earthquake, was obtained, indicating the possibility of precasting soil behavior in future earthquakes at sites where profiling data are available.

Introduction

Experimental data provided by recent large earthquakes, such as the 1994 Northridge earthquake (M_W ~6.7), the 1995 Kobe (M_W ~6.8) and the 2000 Tottori (M_W ~6.7) Japanese earthquakes, the 1999 Chi-Chi (M_W ~7.7) Taiwanese earthquake and others, have shown clear evidence of the nonlinear behavior of subsurface soils in near-fault zones. During the Kobe earthquake, nonlinear soil behavior was identified at sites located within ~16 km from the fault plane, and the content of nonlinear components in the soil response was estimated. It turned out to be rather high, up to ~60% of the whole intensity of the response, at ~2 km from the fault plane and about 10–15% of the intensity of the response at ~16 km from the fault plane (Pavlenko and Irikura, 2005).

This type of analysis and estimations became possible because of the availability of vertical-array records of the Kobe earthquake. Seismic vertical arrays usually contain two, three, or four three-component accelerometers, installed on the surface and at depths down to ~100 or ~200 m, one of the primary motivations for observations with borehole arrays is to understand nonlinear soil response.

Numerical simulation of accelerograms of the Kobe earthquake at depths of the recording-device locations has shown that (1) at least within ~8–10 km from the fault plane, the nonlinearity in the soil response was substantially higher than that stipulated by conventional computer programs of the nonlinear ground-response analysis, and (2) stress–strain relations of different types, depending on the composition of soil layers, their saturation with water, and depth, describe the behavior of the layers. In particular, the behavior of sandy, water-saturated or wet subsurface soils is described by stress–strain relations of "hard" type, declining to the stress axis at large strains. In such soils, amplification of large-amplitude oscillations occurs, which is related to the "hard-type" nonlinearity of the soil response, as at SGK site during the 1995 Kobe earthquake (Pavlenko and Irikura, 2003).

Acceleration records of the Kobe earthquake gave a good illustration of the fact that in strong ground motion, maxima of energy of oscillations at soil sites shift to a lower-frequency domain. This fact was explained by the nonlinearity of the soil response: mutual interactions of spectral components of seismic waves propagating in soil layers lead to redistribution of the energy of oscillations over the spec-

tral band, and the spectra of signals on the surface tend to take the form $E(f) \sim f^{-k}$ (Pavlenko, 2001).

Numerous surface records obtained during the 1999 Chi-Chi (Taiwan) earthquake possess similar features, indicating nonlinearity of the soil response in many places near the fault plane. Although these records can not be analyzed in the same manner as records of the Kobe earthquake, because of the absence of borehole data, we can suppose that certain typical nonlinear distortions occur in seismic waves of similar intensities in subsurface soils.

The Tottori earthquake occurred in the Tottori Prefecture of Japan at approximately 1:30 p.m. on 6 October 2000. The earthquake mechanism was a strike-slip fault, and the fault-rupture plane surface was about 30 km wide by 10 km deep, nearly vertical (86 degrees). This earthquake was recorded by stations of the Kiban-Kyoshin Digital Strong-Motion Seismograph Network (Kik-Net) at 220 sites located at epicentral distances of 7 to 626 km. It resembled the 1995 Kobe earthquake in its magnitude and focal depth and therefore represented a good opportunity to check the conclusions made based on records of the Kobe earthquake.

Acceleration records of the 2000 Tottori earthquake, provided by the Kik-Net stations, show clear evidence of the nonlinearity of soil response at sites located in near-fault zones, such as evident differences in shapes and spectra of records on the surface and at depth, emphasizing low-frequency oscillations on the surface. In this study, we analyze accelerograms of the 2000 Tottori earthquake and reconstruct stresses and strains, induced in soil layers at sites where the nonlinear soil behavior was identified. We estimate reduction of the shear moduli of the soil layers, caused by the strong motion, and discuss transformations of spectra of seismic waves in the soil layers.

Data and Methodology

Figure 1 (derived from the Kik-Net web site) shows the locations of the mainshock of the Tottori earthquake and the Kik-Net stations in the vicinity of the epicenter. The stations contain two accelerometers, installed on the surface and at a depth of ~100 or ~200 m. Simultaneous records of the two devices allow us to simulate the behavior of soil layers from the surface down to the location of the deep device.

For data processing, we chose stations located within ~80 km from the epicenter, where maximum recorded accelerations exceeded 100 Gal, assuming that at larger distances or at smaller accelerations the soil response is linear. The list of the studied Kik-Net stations with their epicentral distances, maximum recorded accelerations, and soil conditions is given in Table 1.

Nonlinear soil behavior was identified at five Kik-Net stations, namely the TTRH02, SMNH01, HRSH06, SMNH03, and HRSH05 stations, located at 7 km, 8 km, 57 km, 57 km, and 80 km from the epicenter, respectively. At other stations, listed in Table 1, either the profiling data were absent, or the thickness of soft subsurface soil layers was less than ~10 m and they were underlaid by dense rock, so that resonant phenomena predominated over nonlinear ones.

We used the Tottori earthquake records, provided by the Kik-Net stations, for the estimation of nonlinear stress–strain relations in soil layers at different depths, from the surface down to ~100 or ~200 m. The method for the estimation of nonlinear stress–strain relations in soil layers, based on vertical array records, is described in detail in Pavlenko and Irikura (2003).

The profiling data, such as the composition of the soil layers, *P*- and *S*-wave velocities, were provided by the Kik-Net web site. At TTRH02, the upper 10.5 m represent sand and gravel (V_S ~210 m/sec); at SMNH01, the upper 12 m are fill soil with sand, gravel, silt, and cobble stone (V_S ~290 m/sec). At both stations, below these layers down to ~100 m, granites, andesites, and basalts are identified with V_S values gradually increasing from 340 m/sec (at 10.5–20 m) to 790 m/sec (at 42–100 m) at TTRH02 and from 550 m/sec (at 12–22 m) to 2800 m/sec (at 54–100 m) at SMNH01. At HRSH06, the upper 6 m represent weathered mudstone (V_S ~170 m/sec), below which mudstones, conglomerates, and granites are found with V_S values increasing from 270 m/sec (at 6–19 m) to 1650 m/sec (at 51–100 m). At SMNH03, the soil profile consists of fill soil, concrete, sand, and gravel with cobble stone (V_S ~240 m/sec) in the upper 7 m and mudstones, sandstones, and porphyrites below with V_S values increasing from 390 m/sec (at 7–14 m) to 1300 m/sec (at 51–100 m). At HRSH05, the upper 7.5 m of surface soil, clay, sand, and gravel (V_S ~280 m/sec) are underplayed by more dense layers of sand and gravel with cobble stone, sandy clays, slates, and diabases with V_S values increasing from 420 m/sec (at 7.5–32.5 m) to 2390 m/sec (at 80–100 m).

For calculations, the soil profiles were divided into two groups of layers, according to the profiling data. At all stations the groups of upper soft layers were distinguished (10.5 m at TTRH02, 12 m at SMNH01, 6 m at HRSH06, 7 m at SMNH03, and 7.5 m at HRSH05), and "hard-type" stress–strain relations were selected to describe the behavior of these layers. To describe the behavior of deeper layers at all the stations, we used stress–strain relations obtained in laboratory experiments by Hardin and Drnevich (1972). We calculated propagation of vertically incident "input" waves (records of the borehole devices) up to the surface; we developed the calculation program was based on the algorithm by Joyner and Chen (1975). In this program, hard-type stress–strain relations and stress–strain relations obtained in laboratory experiments by Hardin and Drnevich (1972) were used to describe the behavior of the upper and lower layers, respectively. Sets of parametric hard-type stress–strain curves (250 curves) were generated, and an item-by-item examination was applied to identify curves showing the best-fit approximation to observed accelerograms on the surface and at depth. To account for temporal changes in the soil behavior, successive 1.5-sec intervals were analyzed; calculations were performed successively, interval by interval.

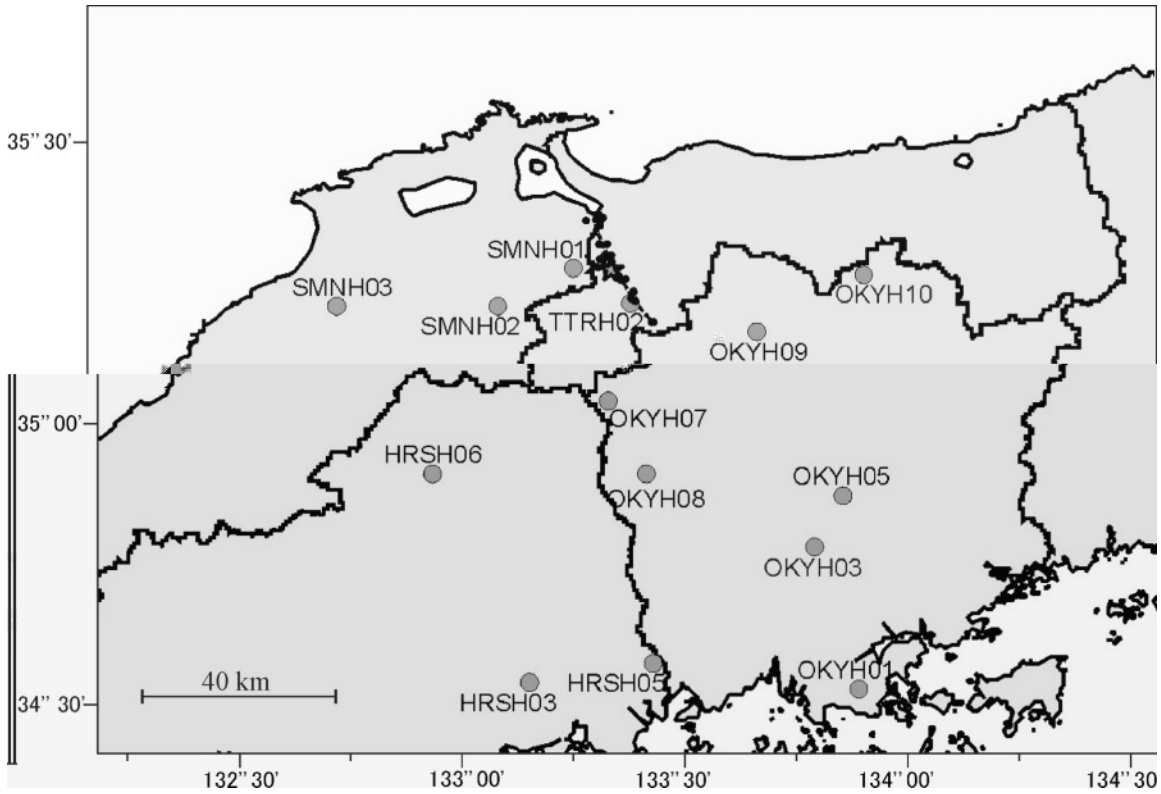

Figure 1. Locations of the mainshock of the 2000 Tottori earthquake and Kik-Net stations in the vicinity of the epicenter (derived from the Kik-Net web site).

Table 1

Maximum Recorded Accelerations, Epicentral Distances, and Soil Conditions at the Kik-Net Stations Located in Near-Fault Zones of the 2000 Tottori Earthquake (Data Derived from the Kik-Net Web Site)

Site Code	Site Name	Maximum Acceleration (Gal)	Epicentral Distance (km)	Thickness of the Upper Soft Soil Layer with V_s <300 m/sec (m)
TTRH02	Hino	927.2	7	11
SMNH01	Hakuta	720.4	8	10
SMNH02	Nita	564.0	24	0
OKYH07	Shingou	179.7	26	0
SMNH10	Mihonoseki	226.4	31	no profiling data
OKYH09	Yubara	283.8	32	0
TTRH04	Akasaki	218.1	33	no profiling data
OKYH08	Tetsuta	238.5	41	0
OKYH14	Hokubou	443.0	45	no profiling data
SMNH12	Yoshida	258.6	46	no profiling data
SMNH11	Hirata	58.2	52	no profiling data
OKYH10	Kamisaibara	280.7	53	8
HRSH06	Kuchiwa	240.3	57	18
SMNH03	Sada	154.8	57	7
OKYH05	Takebe	149.0	65	4
OKYH03	Okayama	129.5	69	7
OKYH11	Syouou	139.1	74	9
SMNH05	Hasumi	121.5	79	4
HRSH05	Kannabe	131.0	80	7

We selected stress–strain relations of the hard type (declining to the stress axis at large strains) to describe the behavior of the upper layers, because at all the stations, except HRSH06, the upper layers represent sandy soils, and *P*-wave velocities indicate the presence of underground water in the upper layers (V_P ~860–900 m/sec at TTRH02 and SMNH01; V_P ~1300–1480 m/sec at SMNH03 and HRSH05, and V_P ~600 m/sec at HRSH06). Evidently, characteristics of oscillations on the surface are defined by the stress–strain relations in the soil layers. Real stress–strain relations of soils obtained in experiments are diverse and depend on the granulometric composition of a soil, its humidity, and so on. In the stress–strain curves of water-saturated soils, the initial convex-up part is followed by a deviation to the stress axis (concave-up part). In such soils (water-saturated sands and clays) possessing hard type of behavior, we can expect shock waves beyond the limit of elasticity (Zvolinskii, 1982), whereas soft soils like loess loams and sands possess stress–strain relations represented by only the convex-up parts, which are often called "soft" diagrams (Zvolinskii, 1982). Thus, hard-type stress–strain relations are typical for water-saturated sandy soils; we used them to describe the behavior of upper soil layers at SGK and TKS sites during the 1995 Kobe earthquake.

At the same time, hard-type stress–strain curves, if defined parametrically, represent the most common case, be-

cause they account for all the features of the soil behavior: in the domain of small strains, these curves are close to linear ones; with increasing strain, they decline to the strain axis, describing "soft" behavior, and, if strains increase more, the curves decline to the stress axis. Therefore, application of our method (and hard-type stress–strain curves) is also possible in cases of quasi-linear soil behavior and in cases of soft soil behavior, if strains are not too large (as at the HRSH06 station). In these cases, the stress–strain relations will be selected that adequately describe the soil behavior in these particular situations.

Because the profiling data provided by the Kik-Net web site contain only the composition of the soil and *P*- and *S*-wave velocities in the layers, we estimated other parameters used in calculations, such as shear stress in failure, τ_{max}, density, and damping in the soil layers. We also defined more exactly *S*-wave velocity profiles at the closest to the fault-plane stations TTRH02 and SMNH01. Density and damping were estimated based on the soil composition. To estimate other profiling parameters, we performed inversion by using the genetic algorithm. For the inversion, we used 20 aftershocks of the Tottori earthquake recorded by the two stations during one month after the mainshock. Intervals defining allowed values of *S*-wave velocities V_S in the soil layers (input data in the inversion problem) included V_S values provided by the Kik-Net web site; limiting estimates of τ_{max} were based on empirical relationships, accounting for the composition of a soil layer, *S*-wave velocity, and pre-existing stress in the layer. For each model (combining V_S and τ_{max} profiling values), we calculated the propagation of the aftershock waves in the soil layers; the behavior of the layers was described by the stress–strain relation obtained by Hardin and Drnevich (1972). All the models were evaluated by the summary deviations of the simulated accelerograms from the recorded ones. The deviations were calculated as sums of the mean square "point-by-point" deviations and the differences of the mean intensities of the simulated and recorded accelerograms. The "best" model was produced after crossing of 50 initial models during about 500 generations.

For the TTRH02 station, the four-layer (as given at the Kik-Net web site) and seven-layer (as proposed by some seismologists) models were considered. Figure 2a shows the V_S profile given on the Kik-Net web site, the best obtained V_S and τ_{max} profiles, and the plots illustrating the decrease of the deviation between the simulated and recorded accelerograms with increasing the generation number for the four-layer and seven-layer models at TTRH02. As seen from Figure 2, the profiling values for both models are similar, and the seven-layer model does not provide any advantages over the four-layer model in simulating the aftershock wave fields. Finally, the best four-layer model, shown in Figure 2a, was selected for further calculations. Figure 2b shows similar results for the SMNH01 station, that is, the V_S profile given at the Kik-Net web site, and the best obtained V_S and τ_{max} profiles.

For the HRSH06, SMNH03, and HRSH05 stations, the profiling data were estimated based on the empirical relationships, accounting for the composition of the soil layers, *S*-wave velocities, and pre-existing stresses in the layers. Based on the profiling data obtained, stresses and strains induced in the soil layers at the five stations during the mainshock of the earthquake were estimated. The obtained stresses and strains were used to trace changes in the shear moduli in the soil layers.

Results

Stresses and strains at depths of 0–100 m or 0–200 m, changing with time during the strong motion, were estimated for TTRH02, SMNH01, HRSH06, SMNH03, and HRSH05 (Figs. 3, 4, 5, 6, 7). As seen from these figures, a good agreement was obtained between the simulated and observed accelerograms for all the stations, though the agreement is worse than that achieved for SGK and TKS sites in simulating accelerograms of the 1995 Kobe earthquake (Pavlenko and Irikura, 2003). Evidently, the accuracy of simulation sufficiently depends on the available information on the parameters of the soil profiles. At SGK and TKS sites, these parameters were measured before and after the Kobe earthquake; 28 and 40 soil layers, respectively, were distinguished at these sites, for which *P*- and *S*-wave velocities and densities were determined and laboratory testing of soil samples was performed, which allowed rather accurate estimations of shear stress in failure, τ_{max}, in the soil layers. At Kik-Net stations, such information is not available, and inversions based on genetic algorithm have not substantially improved our knowledge of the soil parameters. Apparently, the results of simulation shown in Figures 3–7 cannot be improved without additional information on the parameters of the soil profiles.

However, the applied method of simulation allows some correction of the soil parameters. Stress–strain relations used in calculations are defined in their normalized form in the manner proposed by Hardin and Drnevich (1972): stress is normalized by multiplying by $1/\tau_{max}$, and strain is normalized by multiplying by G_{max}/τ_{max}. During the calculations, stress–strain relations are selected that satisfy the prescribed (probably, with some error) values of G_{max} and τ_{max} to simulate oscillations on the surface close to the observed ones. At the same time, the result, that is, vertical distributions of stresses and strains in the soil layers, is expressed in absolute stress and strain units (Figs. 3–7); this decreases its dependence on the selected G_{max} and τ_{max} and allows us to make conclusions about the soil behavior.

At the closest to the fault-plane stations TTRH02 and SMNH01, the soil response was substantially nonlinear, as seen from Figures 3 and 4. At these stations, the behavior of the upper soil layers during the earthquake can not be described by a single stress–strain relation; an agreement between the observations and simulations can only be obtained if we describe the behavior of the upper layers by

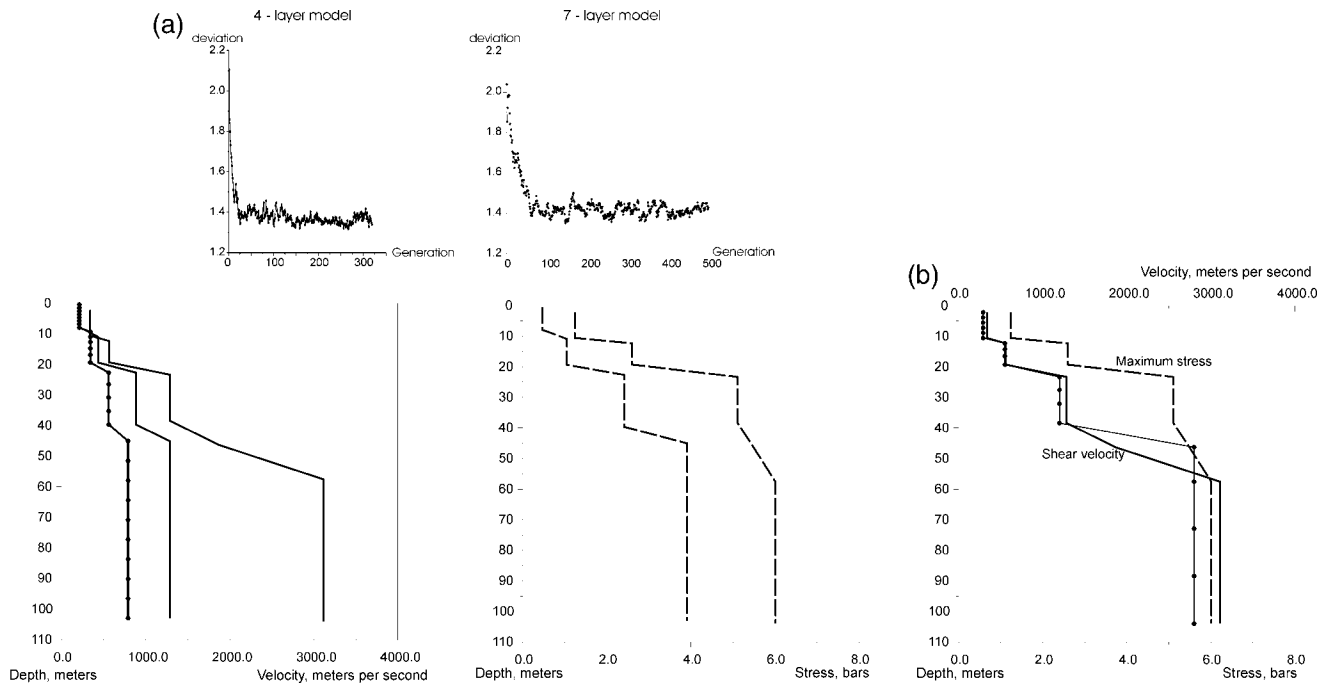

Figure 2. (a) V_S profile, given at the Kik-Net web site (marked by filled circles on the left-hand figure), the best obtained V_S and $\tau_{\max}$ profiles, and the plots, illustrating the decrease of the deviation between the simulated and recorded accelerograms with increasing the generation number for the four-layer and seven-layer models at the TTRH02 station. (b) V_S profile, given at the Kik-Net web site (marked by filled circles) and the best obtained V_S and $\tau_{\max}$ profiles at the SMNH01 station.

different stress–strain relations at different intervals. Thus, strong ground motion changes rheological properties of the upper soil layers in near-fault zones.

As seen from Figures 3 and 4, strains induced by the strong motion achieve 0.6% in the upper 10.5 m at TTRH02 and 0.3% in the upper 12 m at SMNH01. At both stations resonant oscillations in the upper soil layers are observed; maximum stresses are as high as ~0.6 bars in the upper 10–12 m and increase with depth up to ~5 bars at 50–100 m, whereas strains decrease with depth. The shapes of the stress–strain curves in the upper soil layers reveal pore pressure development during the strong motion (Figs. 3 and 4).

At stations HRSH06, SMNH03, and HRSH05, located at epicentral distances of 57 km and more, the behavior of the upper soil layers is described by the same stress–strain relation at all intervals (Figs. 5–7); rheological properties of the soil are not changed. During the 1995 Kobe earthquake, changes of the rheological properties of the upper soil layers were detected at Port Island and SGK sites, located within ~6 km from the fault plane. Thus, records of two earthquakes with magnitudes M_w ~6.7–6.8 and focal depths less than ~30 km allow a rough estimation of the area where the rheological properties of the upper soil layers change, as ~7–8 km, or ~1/4 of the length of the fault. Stresses and strains in the soil layers at these stations are substantially lower than at TTRH02 and SMNH01: up to 0.12 bars and 0.05% in the upper 5–8 m; stresses increase up to ~0.5 bars at 50–100 m (Figs. 5–7).

Also we analyzed records of other stations listed in Table 1. For SMNH02, we could not obtain an agreement between the simulated and observed accelerograms with the V_S profile provided at the Kik-Net web site. The agreement can be obtained if we assume that the V_S in the layers is ~30–80% higher than indicated on the web site. Higher *S*-wave velocities would better correspond to *P*-wave velocities in the layers, and the profiling data would resemble the data at the neighboring station SMNH01. That would be reasonable, because the stations are close to each other, and the earthquake recordings look similar at the two stations. The ground response at stations OKYH07, OKYH08, OKYH09, and OKYH10, where the upper layers represent dense soil with high V_S values, can be simulated, and an agreement between the simulations and observations can be obtained if we describe the behavior of all the soil layers with the stress–strain relation obtained in laboratory experiments by Hardin and Drnevich (1972). At stations OKYH05, OKYH03, OKYH11, and SMNH05, the thickness of the soft soil layer is less than 10 m, whereas the epicentral distances are rather large, and the ground response is virtually linear. Quasi-monochromatic oscillations predominate in records on the surface at these stations, indicating the predominance of resonance effects over nonlinear

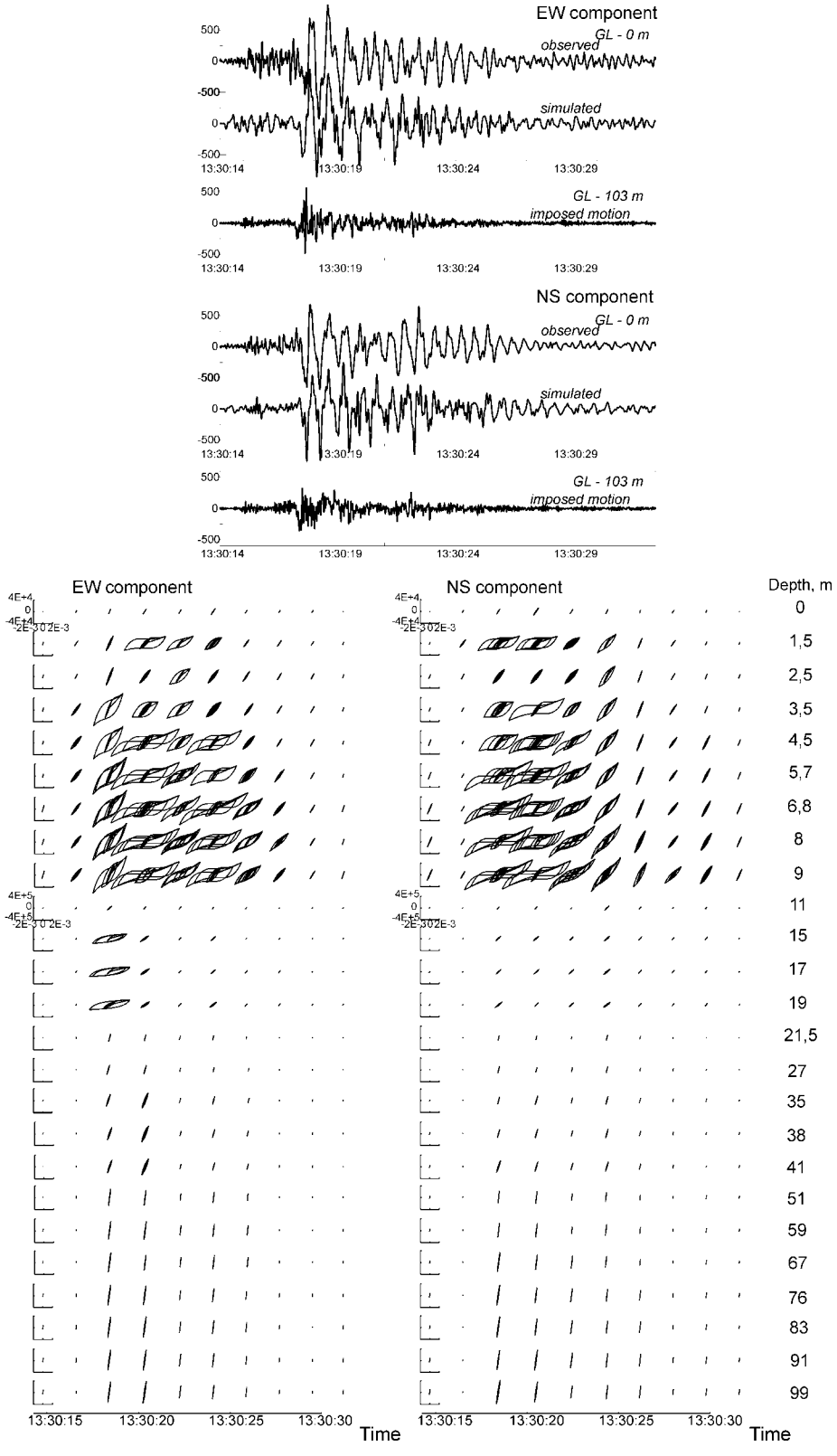

Figure 3. The acceleration time histories of the mainshock of the Tottori earthquake, observed and simulated, and estimated stress–strain relations in the soil layers, changing with time during the strong motion, at the TTRH02 station (stresses are given in Pa; strains, in strains, the same scales for depths 0–10 m and 11–100 m).

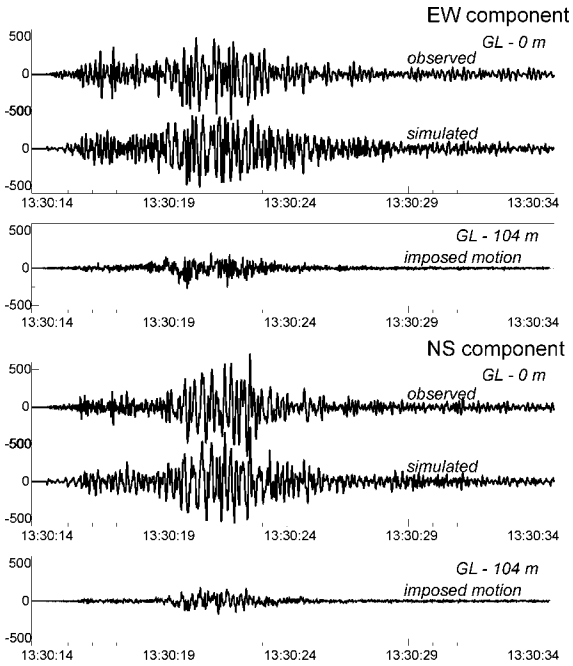

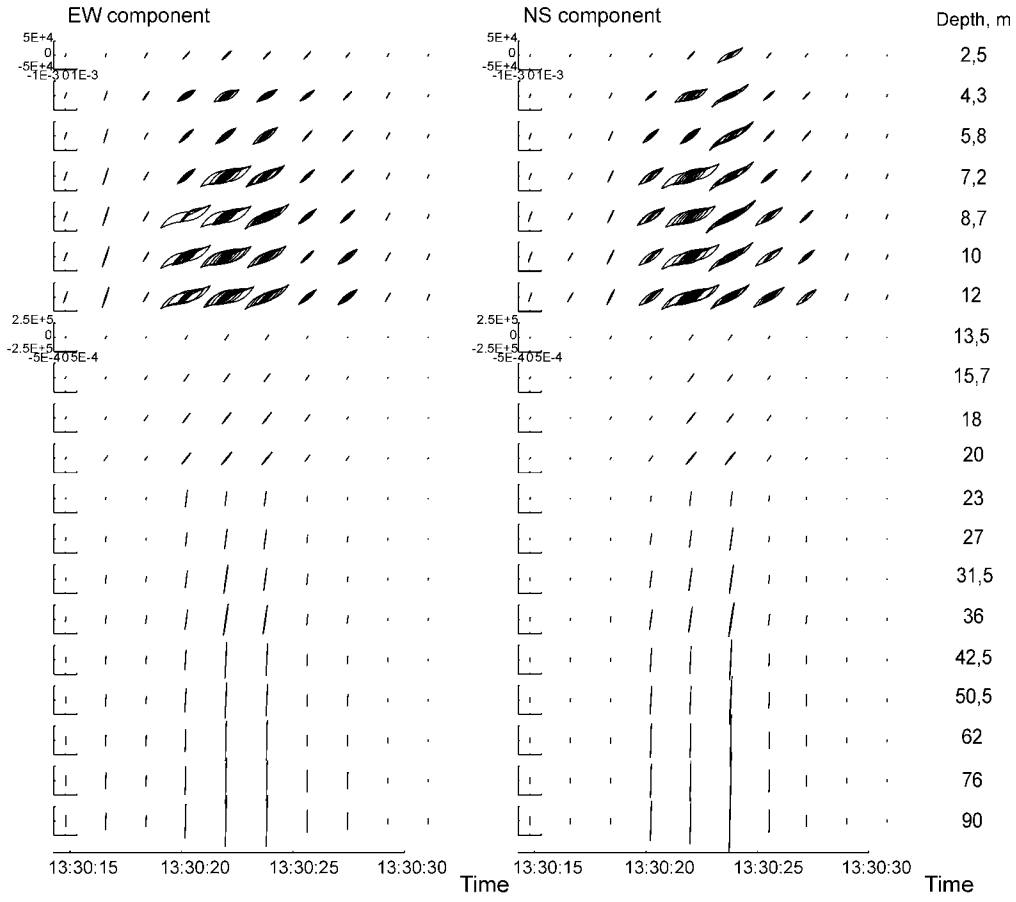

Figure 4. Same as Figure 3 for the SMNH01 station (stresses are given in Pa; strains, in strains, the same scales for depths 0–12 m and 13–100 m).

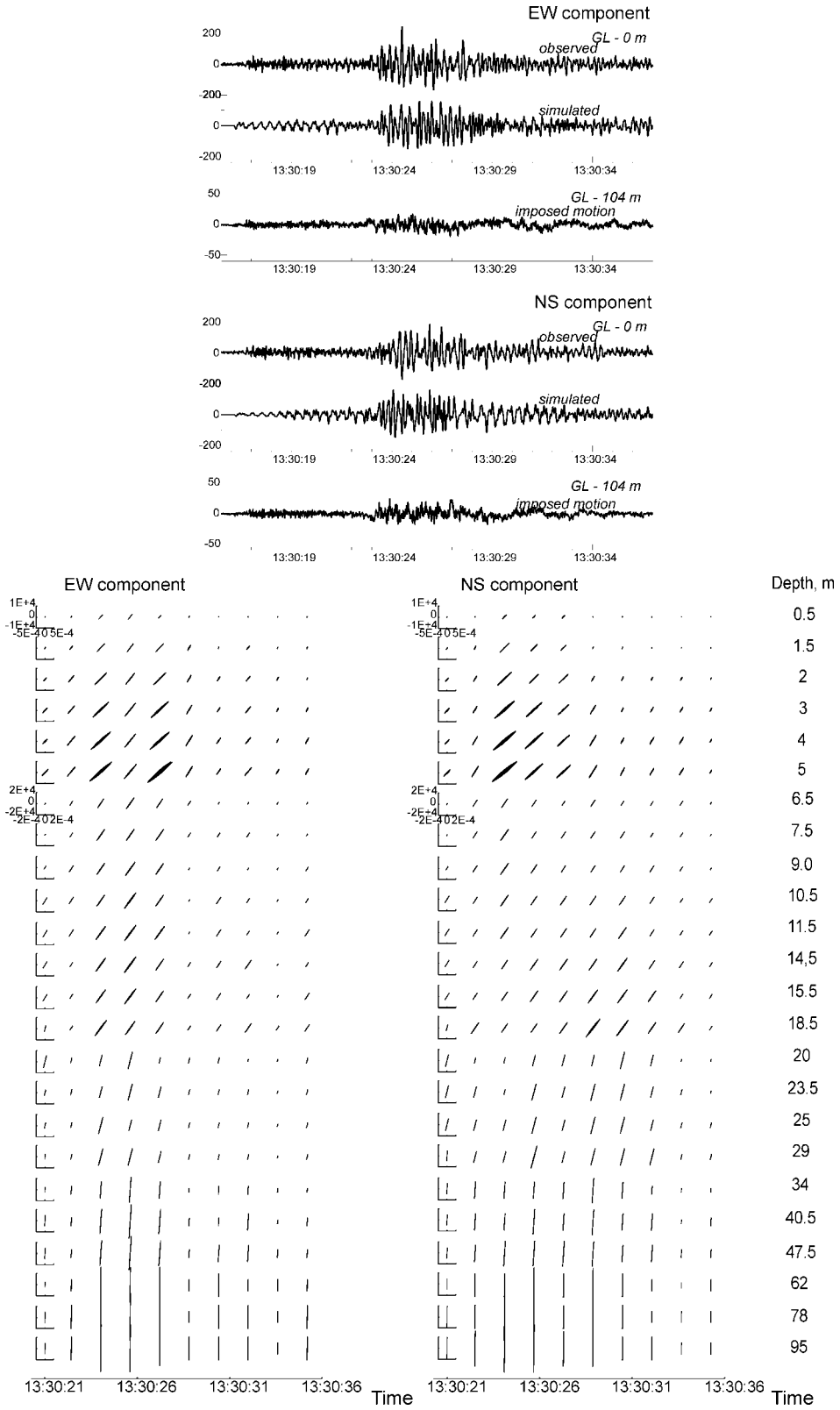

Figure 5. Same as Figure 3 for the HRSH06 station (stresses are given in Pa; strains, in strains, the same scales for depths 0–5 m and 6–100 m).

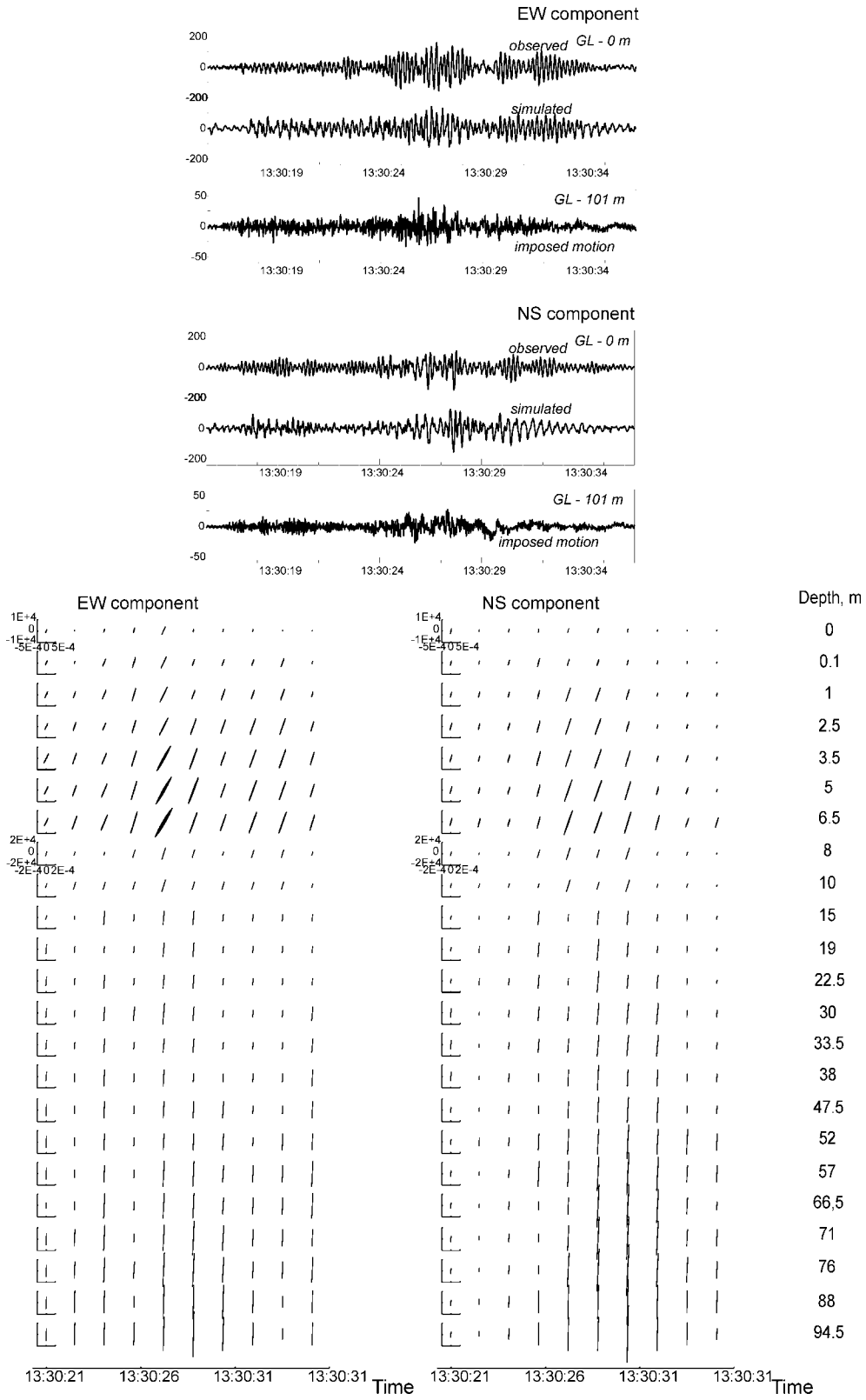

Figure 6. Same as Figure 3 for the SMNH03 station (stresses are given in Pa; strains, in strains, the same scales for depths 0–7 m and 8–100 m).

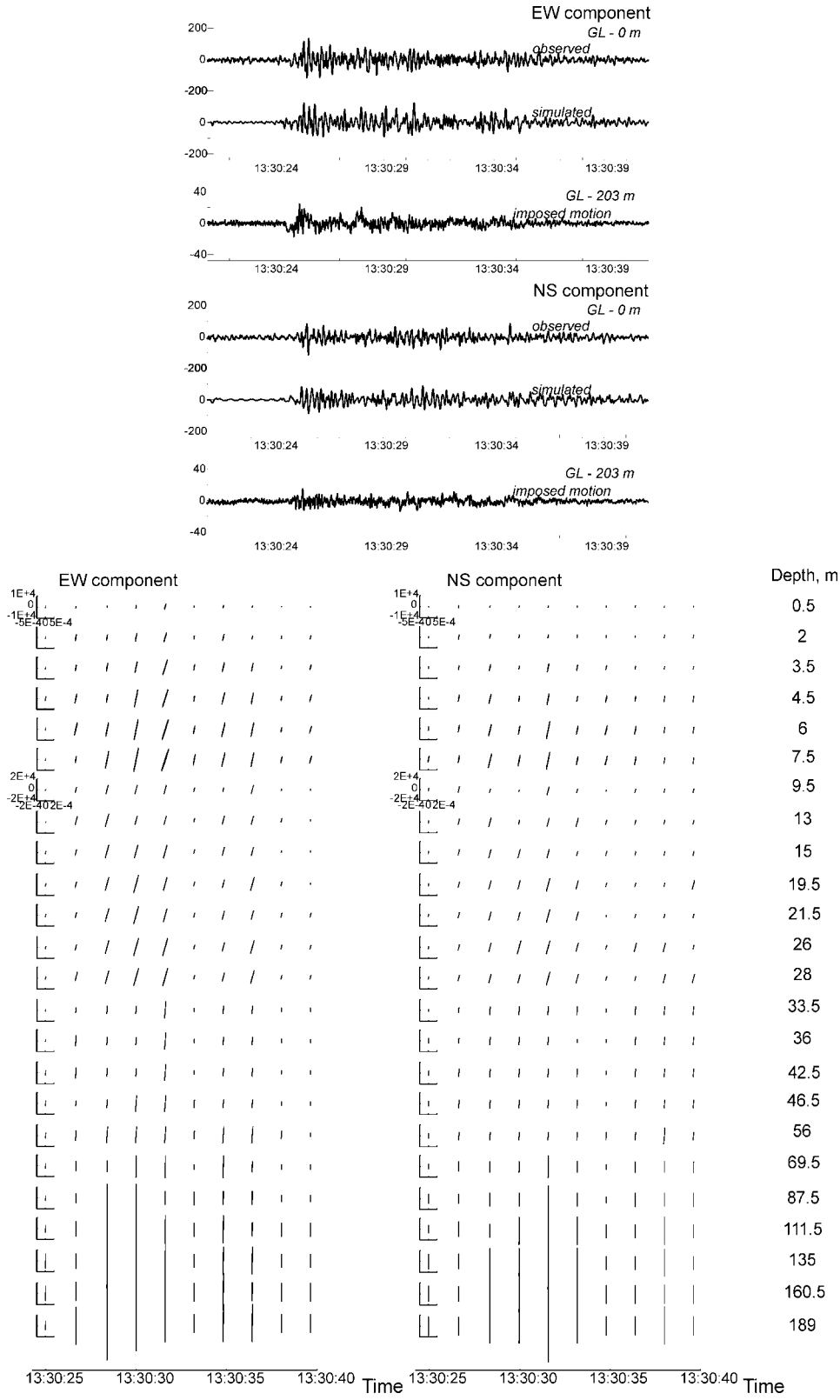

Figure 7. Same as Figure 3 for the HRSH05 station (stresses are given in Pa; strains, in strains, the same scales for depths 0–7 m and 8–100 m).

ones. At these stations, the soil behavior can also be simulated with the stress–strain relation obtained by Hardin and Drnevich (1972).

The estimated stresses and strains, changing with time during the strong motion, were used to trace changes in the shear moduli of the soil layers. As seen from Figures 3–7, these changes are observed in the upper 9–12 m of the soil profiles at the closest to the fault-plane stations. The behavior of the deeper layers at these stations and the behavior of all the layers at remote stations HRSH06, SMNH03, and HRSH05 were stable. Figure 8 represents changes in the shear moduli at the studied Kik-Net stations during the strong motion estimated for both east–west and north–south components. Shear moduli were calculated as slopes of stress–strain curves averaged over the groups of upper layers and over oscillations within each interval during the strong motion. At the TTRH02 and SMNH01 stations, the reduction of the shear moduli in the upper layers achieved ~60% of their initial values, at the HRSH06 station the reduction of the shear moduli did not exceed 15% of the initial value, though scattering does not allow accurate estimation, and at the SMNH03 and HRSH05 stations it was negligible (Fig. 8).

Though scattering of the obtained estimates of shear moduli reduction indicate some inaccuracy in our simulations (which is due to insufficiency of information on the soil parameters, as shown previously), we can see from Figure 8a total recovery of the shear modulus at the TTRH02 station and its almost total recovery at the SMNH01 station. Also, we can see that the recovery starts immediately following the decrease of the intensity of the strong motion (Figs. 3, 4, and 8), which testifies to a high permeability of the upper soil layers as composed of noncohesive soils: sands, gravels, silts with cobble stones. Similar shear modulus behavior was observed at SGK and TKS sites during the 1995 Kobe earthquake (Pavlenko and Irikura, 2002).

Note a significant amplification of low-frequency oscillations on the surface at TTRH02, which is due to the hard-type nonlinearity of the soil response, as seen in Figure 3. A similar tendency is seen in records of the SMNH01 station. At other stations, the thickness of the soft soil layer is rather small, and resonance effects predominate in oscillations on the surface. As a result, transformations of spectra caused by the nonlinearity of the soil response are almost insignificant.

Figure 9 represents acceleration spectra of the Tottori earthquake at some Kik-Net stations. As known, nonlinearity of the soil response induces changes in spectra of seismic waves propagating in the soil layers: the energy of the waves is redistributed over the spectral bands, because of mutual interactions of spectral components of the propagating waves. Low-frequency components are amplified, spectral peaks and spectral gaps are smooth, and spectra of oscillations on the surface tend to take the form $E(f) \sim f^{-k}$. This spectral shape can be achieved in cases of strong nonlinearity (intense seismic waves and/or thick soft soil layers), whereas in cases of weak nonlinearity, we only see the tendencies of these spectral transformations. These tendencies are clearly seen in spectra of the TTRH02 station (Fig. 9). At other stations, however, resonance phenomena prevail, and spectral changes, induced by the soil nonlinearity, are inconspicuous.

Discussion and Conclusions

Thus, we constructed models of the soil behavior in near-fault zones of the 2000 Tottori earthquake. We estimated the stresses and strains induced in the soil layers by the strong motion (Figs. 3–7). Noticeable changes in the shear moduli occurred in the upper layers (9–12 m) at the closest to the fault-plane stations TTRH02 and SMNH01. At these stations, strong ground motion induced changes in the rheological properties of the upper layers. At stations located at epicentral distances of 57 km and more, shear moduli of the soil layers were almost not changed during the earthquake.

A similarity was found in the soil behavior in near-fault zones during the 1995 Kobe earthquake and the 2000 Tottori earthquake, that is, the behavior of soils of similar composition, bedded in similar geotechnical conditions at different sites, is described by similar stress–strain relations. Soils possessing stress–strain relations of the hard type predominate in areas where the level of the underground water is close to the surface. In this case, acceleration amplitudes increase in the upper layers at rather large strains.

As known, there are three basic mechanisms of seismic-wave transformations in soil layers: (1) amplification of oscillations in subsurface layers possessing lower values of seismic velocities and densities; (2) resonance phenomena, also leading to amplification of oscillations on the surface; and (3) nonlinearity of the soil response, usually leading to deamplification of oscillations.

The first two "linear" mechanisms have been studied extensively during past decades, and now they are adequately accounted for in engineering practice. Regarding the third "nonlinear" mechanism, the results obtained in this work allow us to formulate the following conclusions:

First, nonlinearity of ground response leads to changes in spectra and amplification of seismic waves propagating in the soil layers.

Spectral transformations reveal themselves in shifting the resonance frequencies of the soil layers to the low-frequency domain and in tendencies to take the smoothed form $E(f) \sim f^{-k}$. This spectral shape is due to the action of nonlinear damping mechanisms: they weaken spectral components at high and medium frequencies and do not influence low-frequency components. Nonlinear damping mechanisms not depending on the dissipative properties of the medium are due to wasting energy of the propagating waves on generating their higher-frequency harmonics, which are

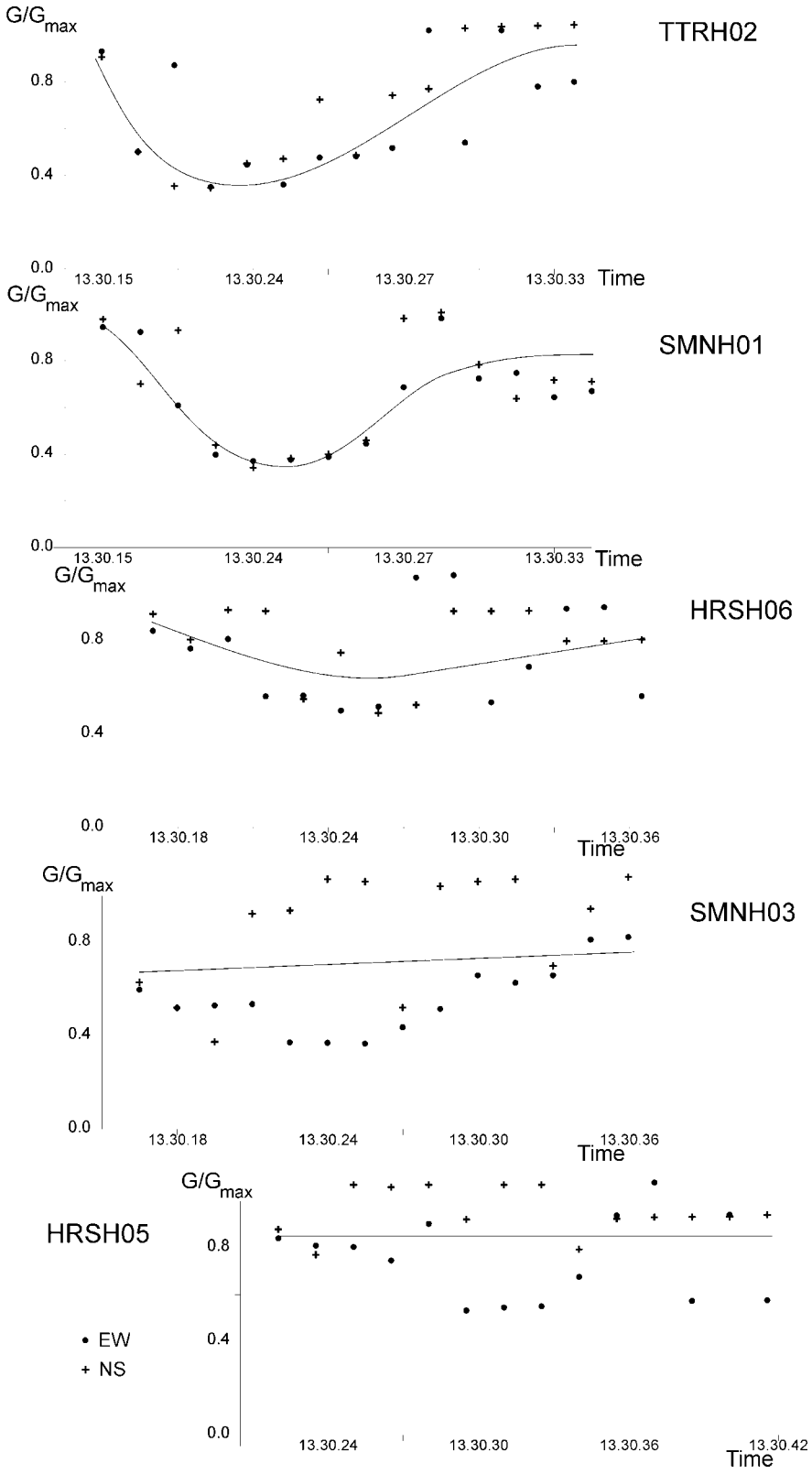

Figure 8. Shear moduli changes of the upper soil layers at the studied stations during the 2000 Tottori earthquake.

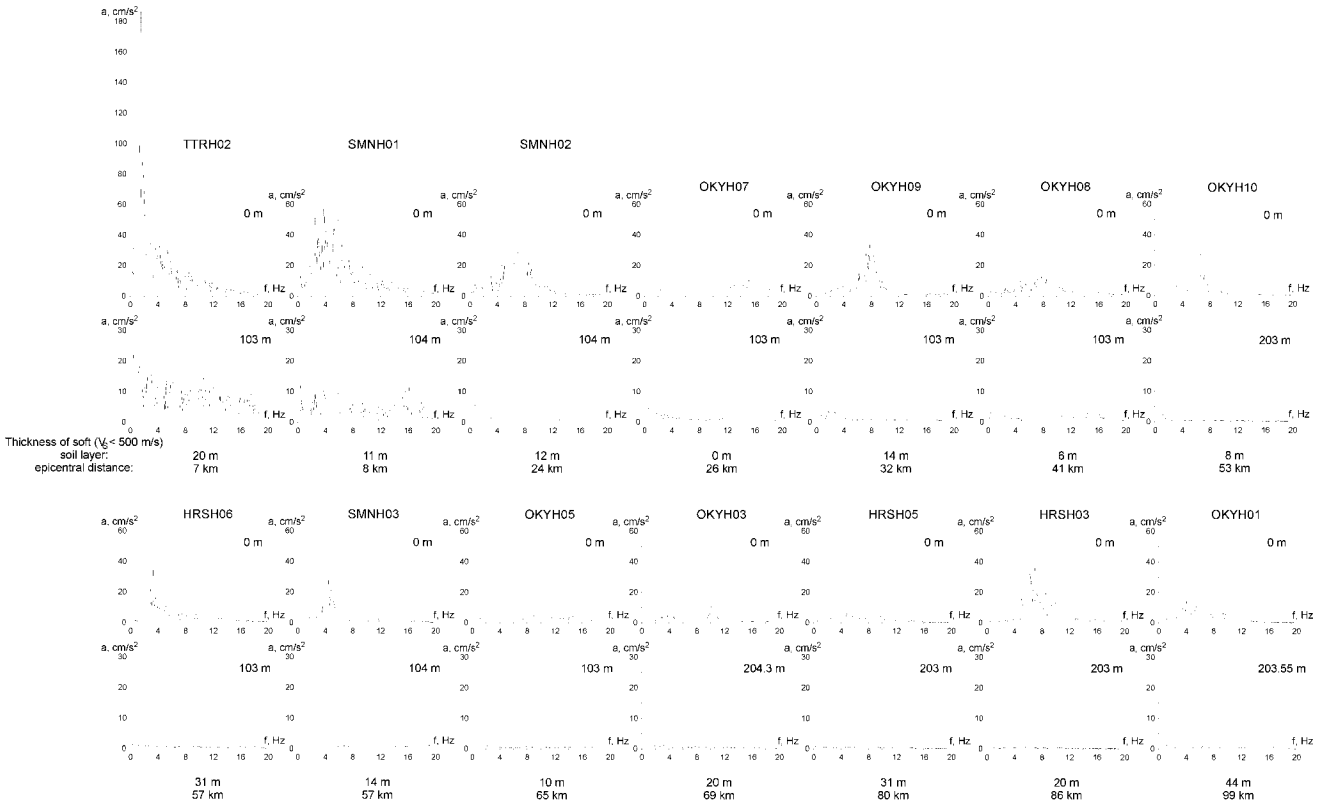

Figure 9. Acceleration spectra of the 2000 Tottori earthquake (north–south and east–west components) at the Kik-Net stations.

damped more quickly than the main-frequency waves, because damping usually increases with frequency (Zarembo and Krasil'nikov, 1966; Rudenko, 1986). In seismology, nonlinear damping is related to the area within hysteretic stress–strain curves; as known, it increases with increasing the intensity of seismic oscillations (Hardin and Drnevich, 1972).

If low-frequency components were reduced or absent at the input of the soil profile, they appear at the output, resulting from nonlinear interactions and generating combination frequencies of "difference type," $f_1 - f_2$; therefore, they can be amplified. At the same time, nonlinear damping does not decrease amplitudes of low-frequency components, and they remain high even in cases of strong nonlinearity of the soil response, as at Kik-Net stations TTRH02 and SMNH01 during the Tottori earthquake and at SGK and TKS sites during the Kobe earthquake (Pavlenko and Irikura, 2003).

Concerning the influence of the soil nonlinearity on amplification of seismic waves in subsurface soil layers, we should distinguish two cases, namely "soft" and "hard" types of nonlinearity (stress–strain relations), which were described previously.

Sometimes nonlinearity of the soil behavior is unambiguously connected to deamplification of oscillations on the surface; decrease of amplification of intense seismic waves compared with weak ones in soil sites is treated as an indicator of soil nonlinearity (Beresnev *et al.*, 1995; Field *et al.*, 1997). However, our results show that this is true only in cases of soft-type nonlinearity, when the behavior of the upper layers is described by soft-type stress–strain relations, declining to the strain axis at large strains; usually, this corresponds to cases when the level of the underground water is below ~10 m. An example is the Port Island site (Pavlenko and Irikura, 2003). If the behavior of the upper soil layers is described by hard-type stress–strain relations (usually, in cases when the level of the underground water is above ~10 m), amplification of oscillations on the surface occurs at rather high strains. TTRH02 and SMNH01 possess this type of nonlinearity, as well as the SGK and TKS sites during the Kobe earthquake (Pavlenko and Irikura, 2003). The mechanism of amplification is illustrated by Figures 3 and 4: at large strains, stress–strain relations in the upper layers decline to the stress axis, and amplitudes of low-frequency oscillations increase.

In articles by Dimitriu *et al.* (2000) and Dimitriu (2002), statistical analysis of weak- and strong-motion records has shown that at resonant sediment sites, deamplification was restricted to a limited frequency band, below which the nonlinear (strong-motion) response exceeded the linear (weak-motion) one. At the same time, Yu *et al.* (1992) showed by numerical simulation of strong-motion accelerograms at soil

sites that nonlinearity does not affect spectral amplitudes in the lowest frequency range, decreases amplitudes in the central band, and slightly increases spectral amplitudes in the high-frequency range.

Dimitriu *et al.* (2000) and Dimitriu (2002) do not describe soil conditions at the observation sites, and according to our conclusions, we can suppose the "hard" type of soil behavior at these sites. Only, in this case, the nonlinear soil response can exceed linear one.

Note that the problem of seismic-wave amplification and transformation of their spectra in the soil layers is rather complicated, and we are preparing a separate article dealing with this problem and referring to the results of the statistical nonlinear acoustics. In this article, we wanted to emphasize that changes in spectra and amplification of seismic waves in subsurface soils at Kik-Net stations TTRH02 and SMNH01 during the Tottori earthquake, as well as at stations SGK and TKS during the Kobe earthquake (Pavlenko and Irikura, 2003), represent good illustrations of the earlier stated regularities.

Second, in cases when the thickness of subsurface soft soil layers is less than ~20 m, resonance phenomena usually predominate over nonlinear ones. Nonlinearity of soil response stipulates the dependence of resonance frequencies on the intensity of seismic oscillations. Therefore, any presumable estimates of frequency-dependent amplification factors are not correct; a correct approach is calculation of the ground response in concrete situations.

Third, maximum strains are usually induced at the bottom of subsurface soft layers; they correspond to low-frequency oscillations, caused by the soil nonlinearity. This should be considered in constructing underground structures.

Based on processing records of the 1995 Kobe and 2000 Tottori earthquakes, we can formulate the limitations of conventional computer programs of ground-response analysis (i.e., widely used programs in which the behavior of all soil layers is described in a similar manner: SHAKE, FDEL, CHARSOIL, NONLI3, EERA, NERA, etc.): (1) disregard of the differences in the behavior of separate soil layers during strong ground motion and (2) ignoring of changes in rheological properties of the upper soil layers, induced by the strong motion.

According to our estimations, based on records of the Kobe (1995) and Tottori (2000) earthquakes, during crustal earthquakes with magnitudes M_w ~6.7–6.8, strong nonlinearity of the soil response (changes in rheological properties of the upper soil layers and shear modulus reduction of ~50–60% and more) are observed within an area up to ~7–8 km from the fault plane (~one-fourth of the length of the fault). Within this area, noticeable manifestations of soil nonlinearity are observed in the upper 15–25 m of the soil profiles. At distances of ~15 km from the fault plane (~ one-half of the length of the fault), nonlinearity is much weaker, even in soft subsurface soils. Stress–strain relations, suggested by Hardin and Drnevich (1972), adequately describe the behavior of soils at all depths in conditions of moderate dynamic loadings. In conditions of large loadings, in cases of strong nonlinearity, these stress–strain relations can be used to describe the behavior of dense soils at depths below some level (15–25 m for Kobe and Tottori earthquakes), depending on the composition of the soil layers and their saturation with water, as well as on the magnitude and location of the earthquake; whereas the behavior of soft subsurface soils should be described by other, more "nonlinear" stress–strain relations. Such relations are found in this work.

Ignoring the features of soil behavior in strong ground motion leads to underestimation of maximum acceleration in near-fault zones and mistaken estimates of spectra of oscillations on the surface at soil sites.

Acknowledgments

We thank L. F. Bonilla and an anonymous reviewer for their valuable comments and suggestions. We also thank the web site of the Kik-Net Digital Strong-Motion Seismograph Network, www.kik.bosai.go.jp, for records of the 2000 Tottori earthquake and profiling data.

References

Beresnev, I. A., K.-L. Wen, and Y. T. Yeh (1995). Nonlinear soil amplification: its corroboration in Taiwan, *Bull. Seism. Soc. Am.* **85,** 496–515.

Dimitriu, P. P. (2002). The HVSR technique reveals pervasive nonlinear sediment response during the 1994 Northridge earthquake (M_w 6.7), *J. Seism.* **6,** 247–255.

Dimitriu, P. P., N. Theodulidis, and P.-Y. Bard (2000). Evidence of nonlinear site response in SMART-1 (Taiwan) data, *Soil Dyn. Earthquake Eng.* **20,** 155–165.

Field, E. H., P. A. Johnson, I. A. Beresnev, and Y. Zeng (1997). Nonlinear ground-motion amplification by sediments during the 1994 Northridge earthquake, *Nature* **390,** no. 6660, 599–602.

Hardin, B. O., and V. P. Drnevich (1972). Shear modulus and damping in soils: design equations and curves, *Proc. ASCE, J. Soil Mech. Found. Div.* **98,** 667–692.

Joyner, W. B., and T. F. Chen (1975). Calculation of nonlinear ground response in earthquakes, *Bull. Seism. Soc. Am.* **65,** 1315–1336.

Pavlenko, O. V. (2001). Nonlinear seismic effects in soils: numerical simulation and study, *Bull. Seism. Soc. Am.* **91,** no. 2, 381–396.

Pavlenko, O. V., and K. Irikura (2002). Changes in shear moduli of liquefied and nonliquefied soils during the 1995 Kobe earthquake and its aftershocks at PI, SGK, and TKS vertical array sites, *Bull. Seism. Soc. Am.* **92,** no. 5, 1952–1969.

Pavlenko, O. V., and K. Irikura (2003). Estimation of nonlinear time-dependent soil behavior in strong ground motion based on vertical array data, *Pure Appl. Geophys.* **160,** 2365–2379.

Pavlenko, O. V., and K. Irikura (2005). Identification of the nonlinear behavior of liquefied and nonliquefied soils during the 1995 Kobe earthquake, *Geophys. J. Int.* **160,** 539–553.

Rudenko, O. V. (1986). Interactions of intense noise waves, *Sov. Phys. Uspekhi* **29,** no. 7, 620–641.

Yu, G., J. G. Anderson, and R. V. Siddharthan (1993). On the characteristics of nonlinear soil response, *Bull. Seism. Soc. Am.* **83,** 218–244.

Zarembo, L. K., and V. A. Krasil'nikov (1966). *Introduction to Nonlinear Acoustics*, Nauka, Moscow.

Zvolinskii, N. V. (1982). Wave processes in non-elastic media, *Prob. Eng. Seism.* **23,** 4–19.

Institute of Physics of the Earth
Russian Academy of Sciences
B. Gruzinskaya 10
Moscow 123995, Russia
olga@ifz.ru
(O.V.P.)

Earthquake Motion Research Institute
4-3-2 Itachibori, Nishi-ku
Osaka, 550-0012, Japan
irikura@geor.or.jp
(K.I.)

Manuscript received 25 March 2006.